Bioconjugate Chemistry

Article

pubs.acs.org/bc

Highly Reactive *trans*-Cyclooctene Tags with Improved Stability for Diels–Alder Chemistry in Living Systems

Raffaella Rossin,[†] Sandra M. van den Bosch,[†] Wolter ten Hoeve,[‡] Marco Carvelli,[†] Ron M. Versteegen,[§] Johan Lub,[†] and Marc S. Robillard*[,†]

[†]Philips Research, Eindhoven, The Netherlands

[‡]Syncom BV, Groningen, The Netherlands

[§]SyMO-Chem BV, Eindhoven, The Netherlands

Supporting Information

ABSTRACT: One of the challenges of pretargeted radioimmunotherapy, which centers on the capture of a radiolabeled probe by a preinjected tumor-bound antibody, is the potential immunogenicity of biological capturing systems. A bioorthogonal chemical approach may circumvent this drawback, but effective in vivo chemistry in mice, larger animals, and eventually humans, requires very high reagent reactivity, sufficient stability, and retained selectivity. We report here that the reactivity of the fastest bioorthogonal reaction, the inverse-electron-demand-Diels–Alder cycloaddition between a tetrazine probe and a *trans*-cyclooctene-tagged antibody, can be increased 10-fold (k_2 = 2.7 × 10^5 M^{-1} s^{-1}) via the *trans*-cyclooctene, approaching the speed of biological interactions, while also increasing its stability. This was enabled by the finding that the *trans*-cyclooctene tag is probably deactivated through isomerization to the unreactive *cis*-cyclooctene isomer by interactions with copper-containing proteins, and that increasing the steric hindrance on the tag can impede this process. Next, we found that the higher reactivity of axial vs equatorial linked TCO can be augmented by the choice of linker. The new, stabilized, and more reactive tag allowed for improved tumor-to-nontumor ratios in pretargeted tumor-bearing mice.

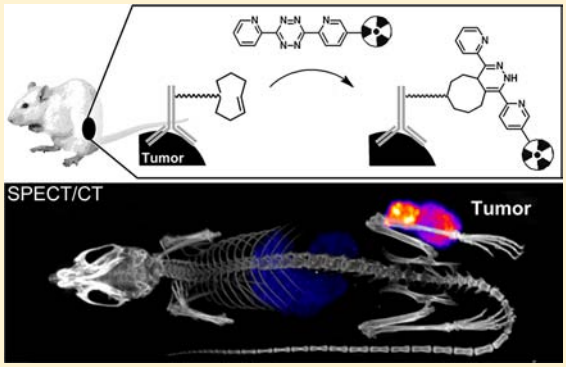

INTRODUCTION

The emergence of bioorthogonal chemical reactions has unearthed a wealth of exciting new possibilities for probing and manipulating biological systems.[1−3] For noninvasive chemical procedures in mammalian disease models, larger animals, and ultimately humans, there is the need for very fast reaction kinetics to tackle pharmacokinetic challenges such as low target and reagent concentrations, uptake barriers, and reagent clearance. This is especially important for applications that use low amounts of the secondary probe, such as in pretargeted nuclear imaging and radioimmunotherapy (RIT), where a preinjected tumor-bound antibody (mAb) captures a radiolabeled probe, enabling higher tumor-to-nontumor (T/NT) ratios and tumor radiation doses compared to directly radiolabeled antibodies.[4−8] The current clinically validated pretargeting systems use noncovalent biological interactions (streptavidin–biotin, antibody–hapten) to recruit the probe to the tumor-bound mAb, but suffer from immunogenicity and/or involve extensive reengineering and perturbation of the parent mAb. A chemical pretargeting approach enables straightforward antibody modification with small tags and is less likely to give rise to immunogenicity, potentially allowing treatment fractionation. In 2008, Fox and co-workers reported the very fast reaction kinetics (k_2 = 2.0 × 10^3 M^{-1} s^{-1} in MeOH/H_2O (9:1)) and in vitro bioorthogonality of the inverse-electron-demand Diels–Alder (inv-DA) reaction between *trans*-cyclooctene (TCO) and electron-deficient tetrazines,[9] which has led to several very promising bioconjugation applications.[2,10−13] We previously demonstrated that the application of this reaction can be extended to a living animal in a proof of principle tumor pretargeting study (Figure 1):[14] mice were treated with TCO-conjugated CC49 mAb (targeting the pan-adenoma TAG-72 antigen),[15] followed one day later by efficient and selective on-tumor reaction with a small ^{111}In-labeled DOTA-tetrazine probe. Recently, Weissleder and co-workers reported the in vivo use of a tetrazine probe by virtue of its extended circulation time through polymer conjugation.[16] While the high reaction constant of the system used in our pretargeting study (k_2 = 2.7 × 10^4 M^{-1} s^{-1} in PBS)[17] allowed for the efficient capture of a small fast clearing probe, the reactivity was still significantly lower than the association constants of the noncovalent high affinity interactions (5 × 10^5 to 7.5 × 10^7 M^{-1} s^{-1})[7,18−20] used successfully in humans (i.e., at lower concentrations). In addition, the highly strained mAb-

Received: March 26, 2013
Revised: May 23, 2013
Published: June 1, 2013

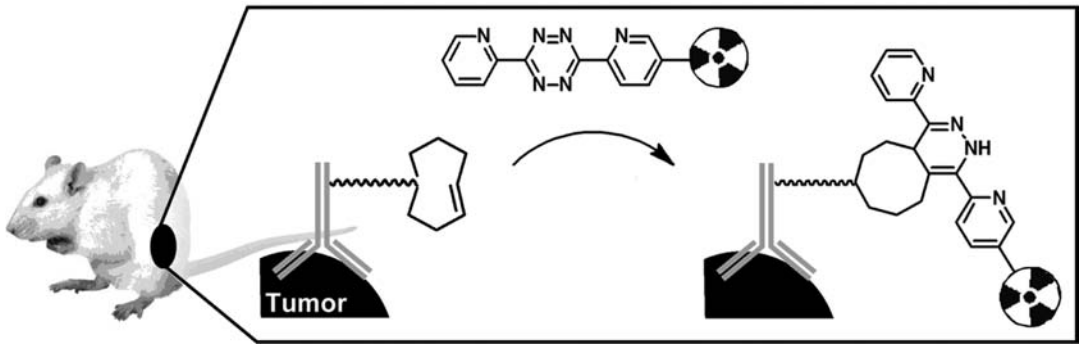

Figure 1. Tumor pretargeting with inverse-electron-demand-Diels–Alder cycloaddition in live mice.

conjugated TCO tag was prone to slow in vivo deactivation (25% in 24 h),[14] limiting the interval between mAb and probe administration. We set out to approach the association rates of the clinically validated biological pretargeting interactions with fast bioorthogonal organic chemistry through improved ring strain-based reactivity of the TCO, while maintaining or increasing the in vivo stability.

EXPERIMENTAL SECTION

General. All reagents and solvents were obtained from commercial sources (Sigma-Aldrich, Acros, ABCR, Invitrogen, and Merck for reagents, Biosolve, Merck and Cambridge Isotope Laboratories for normal and deuterated solvents) and used without further purification unless stated otherwise. [^{177}Lu]Lutetium chloride, [^{111}In]indium chloride, and sodium [^{125}I]iodide solutions were purchased from PerkinElmer. The labeling buffers and PBS were treated with Chelex-100 resin (BioRad Laboratories) overnight, then filtered through 0.22 μm and stored at 4 °C. Mouse serum was purchased from Innovative Research or prepared in house from fresh mouse blood and immediately frozen at −20 °C. Mouse serum albumin (MSA) was purchased from Innovative Research. Analytical radio-HPLC was carried out on an Agilent 1100 system equipped with a Gabi radioactive detector (Raytest). The samples were loaded on an Agilent Eclipse XDB-C_{18} column (4.6 × 150 mm, 5 μm particles), which was eluted at 1 mL/min with a linear gradient of acetonitrile in water containing 0.1% TFA (Gradient for **8a**: 53% MeCN for 10 min, 53–95% MeCN in 1 min, 95% MeCN for 2 min; Gradient for **8b**: 65% MeCN for 2 min, 65–95% MeCN in 5 min, 95% MeCN for 2 min). The UV wavelength was preset at 254 nm. Size exclusion chromatography (SEC) was carried out on an Agilent 1200 system equipped with a Gabi radioactive detector. The samples were loaded on a BioSep-SEC-S 3000 column (300 × 7.8 mm, 5 μm particles, Phenomenex) and eluted with PBS pH 7.4 at 1 mL/min. The UV wavelength was preset at 260 and 280 nm. IEF analysis and SDS-PAGE were performed on a Phastgel system using IEF-3–9 gels and 7.5% PAGE homogeneous gels (GE Healthcare Life Sciences), respectively. The IEF calibration solution (broad pI, pH 3–10) was purchased from GE Healthcare and the protein MW standard solution (Precision Plus dual color standard) was purchased from BioRad. The radioactivity distribution on TLC plates and IEF/SDS-PAGE gels was evaluated with a phosphor imager (FLA-7000, Fujifilm) with the AIDA software (Raytest). The ^{111}In- and ^{177}Lu-labeling yields were determined by radio-TLC, using ITLC-SG strips (Varian Inc.) eluted with 200 mM EDTA in saline. In these conditions, free ^{111}In and ^{177}Lu migrate with R_f = 0.9, while ^{111}In/^{177}Lu-tetrazine remains at the origin. The ^{125}I-labeling yields were also determined with radio-TLC, using ITLC-SG strips eluted with a 1:1 MeOH/EtOAc mixture. In these conditions, free ^{125}I and ^{125}I-SHPP migrate with R_f = 0.5–0.9, while ^{125}I-mAbs remain at the origin. The concentration of CC49 solutions was determined with a NanoDrop 1000 spectrophotometer (absorbance at 280 nm; Thermo Fisher Scientific) or with a BCA test. In the TCO degradation experiment in vitro, the samples incubated at 37 °C for >6 h were topped with mineral oil to avoid sample evaporation.

Syntheses of Pretargeting Components. TCO **10** (exo isomer) was prepared analogously to published procedures.[21] Synthesis of DOTA-tetrazine (**13**) and TCOs **1a** and **2a**, CC49 production, and the conjugation procedure used for CC49-TCO (**1**–**7**, **10**) has been described elsewhere.[14] The synthesis and characterization of all other compounds used herein, radiochemistry, and more experimental details are reported in the Supporting Information.

In Vitro Stability of Model TCOs. The stability of the model TCO **8a**,**b** was evaluated in PBS, 50% mouse serum (purchased from Innovative Research, as well as freshly produced in house) in PBS, and in PBS solutions of MSA and metal-depleted (MD; see below) MSA (21.7 mg/mL), ceruloplasmin (0.2 mg/mL), human transcuprein (α-2-macroglobulin) (0.9 mg/mL), transferrin (1.4 mg/mL), and vitamin B12 (0.3 ng/mL). In a preliminary set of experiments, 100 μM solutions of **8a**,**b** (TCO) and **9** (CCO) in PBS and 50% mouse serum were incubated at 37 °C in the dark under gentle mixing. At t = 0, 3, and 24 h, 100 μL aliquots of the solutions were withdrawn, combined with 100 μL ice-cold MeCN, vortexed for 10 s, filtered through 0.22 μm, and analyzed by RP-HPLC and LC-MS (Supporting Information, Figure S9–S11).

The degradation kinetics of **8a**,**b** was further investigated by analytical RP-HPLC. At selected time points (from 10 min to 7 days incubation at 37 °C), 15 μL aliquots were withdrawn, combined with 15 μL ice-cold MeCN, vortexed for 10 s, and centrifuged at 12,800 rpm for 5 min, after which the supernatants were gently aspirated and analyzed by RP-HPLC. The stability of **8a**,**b** was derived from the ratio of the TCO and CCO peak areas in the UV profiles of the HPLC chromatograms (Supporting Information Figure S12–S13).

Metal Depleted Albumin and Complexes. A 16 mg/mL MSA solution in PBS was dialyzed at 4 °C against 0.1 mM DTPA in PBS (4 days with 4 buffer exchanges) followed by metal-free PBS (2 days with 2 buffer exchanges) in a dialysis cassette (Slide-A-Lyzer, 10 kDa MW cutoff).[22−24] After dialysis, the solution was concentrated to half its volume (Amicon Ultra-4, 10 kDa MW cutoff) and the content of MD-MSA was

dx.doi.org/10.1021/bc400153y | Bioconjugate Chem. 2013, 24, 1210–1217

determined by BCA assay. Two aliquots of the MSA solution (25 mg each) were then complexed with 1 molar equiv $CuCl_2$ or $ZnCl_2$, respectively, by slow addition of 1 mg/mL stock solutions in mQ water, following established procedures,[25−27] which have been shown to afford albumin with respectively Cu bound to its N-terminal binding site and Zn bound to the so-called high affinity zinc site.[26] During the metal addition, the pH was maintained at 7.4 by addition of 0.1 M NaOH. After 1 h incubation at 37 °C, the residual free metal was eliminated by using Amicon Ultra-4 devices (10 kDa MW cutoff). The metal-added MD-MSA was then reconstituted in metal-free PBS and the concentration was determined by BCA assay. The Cu and Zn content in native MSA, MD-MSA, and the metal-added MD-MSA samples was determined by ICP-MS (Element XR High Resolution-Inductively Coupled Plasma-Mass Spectrometer from Thermo Scientific, Supporting Information Table S1).

Radiochemistry. DOTA-tetrazine (**13**) was dissolved (2 mg/mL) in 0.2 M NH_4OAc buffer pH 7.0 and stored at −80 °C before use. An aliquot of **13** was mixed with a suitable amount of [^{177}Lu]lutetium chloride or [^{111}In]indium chloride in 0.2 M NH_4OAc pH 5.5 and incubated at 60 °C for 5 min. The labeling solution (20−50 μL) was then mixed with a 10 mM DTPA solution (5 μL) and incubated for 5 min more. The radiochemical yield (>99%) and radiochemical purity (>95%) were assessed by radio-TLC and radio-HPLC, respectively, after which the labeling mixture was diluted with NH_4OAc pH 5.5 for in vitro experiments or with sterile saline for animal experiments. To avoid potential interference by TCO in the Iodogen labeling method, radio-iodination of CC49-TCO constructs was performed with the Bolton-Hunter method following the manufacturer's instructions. Briefly, an adequate amount of sodium [^{125}I]iodide in 50 μL PBS was mixed with 0.1 μg of Bolton-Hunter reagent (SHPP, Pierce) and 100 μg chloramine-T (N-chloro 4-methylbenzenesulfonamide, sodium salt). The resulting solution was mixed for 10−20 s, after which ^{125}I-SHPP was extracted in toluene and the organic solution was evaporated to dryness under a gentle stream of N_2. CC49-TCO (0.1 mg in 50 μL PBS) was added to the dry ^{125}I-SHPP, the pH was adjusted to 9 with 1 M sodium carbonate buffer, and the reaction mixture was incubated at room temperature for 30−60 min under gentle shaking. After incubation, the labeling yield was determined by radio-TLC. The ^{125}I-labeled mAb was purified twice though Zeba spin desalting columns (40 kDa MW cutoff, Pierce) and the radiochemical purity of the ^{125}I-CC49-TCO solution was determined by radio-TLC, SEC, and SDS-PAGE. Typically, greater than 60% ^{125}I-SHPP conjugation to the mAb and greater than 98% radiochemical purity for the purified ^{125}I-CC49-TCO species were obtained with this procedure. For animal experiments, the specific activity of the ^{125}I-CC49-TCO was adjusted to 2−4 kBq/μg by adding nonradioactive CC49-TCO.

In Vitro Stability of mAb-Conjugated TCOs. 3.3 μM ^{125}I-labeled CC49 and CC49-TCO (**1a**) were incubated in 50% fresh mouse serum (in PBS) at 37 °C in the dark under gentle shaking. At selected times (0, 1, 24, and 48 h) an aliquot of the solutions was diluted 1:10 with PBS and analyzed by IEF and SDS-PAGE followed by phosphor imager (Supporting Information Figure S15 and S16). The pI and MW of the two radioactive species were estimated by comparing the gel radiograms to those obtained with (^{125}I)CC49, (^{125}I)CC49-TCO (**1a**), and pI/MW calibration standards in PBS (Supporting Information Figure S17). Additional in vitro stability experiments can be found in the Supporting Information (Table S3).

In Vitro TCO Reactivity. The reaction constants for CC49-TCO (**1**−**7**, **10**) were measured as previously described (Supporting Information Figure S18).[14] The reaction constant of trans-cyclooct-4-enol **11** with tetrazine **14** in water and acetonitrile at 20 °C was determined by UV absorbance (λ = 320 nm) (Supporting Information Figure S19). The in vitro reactivity of CC49-TCO (**2a,b**) was evaluated by reacting diluted solutions of the mAbs (10, 1, 0.1, 0.01 μM TCO) in PBS with equimolar amount of carrier-added ^{177}Lu-tetrazine **13** for 1 min at 37 °C followed by SDS-PAGE analysis (Supporting Information Figure S20).

Animal Experiments. All animal experiments were performed according to the principles of laboratory animal care (NIH publication 85−23, revised 1985) and the Dutch national law "Wet op de Dierproeven" (Stb 1985, 336). The in vivo experiments were performed in tumor-free or tumor-bearing nude female Balb/C mice (20−25 g body weight, Charles River Laboratories). The human colon cancer cell line LS174T was obtained from the ATCC and maintained in Eagle's minimal essential medium (Sigma) supplemented with 10% heat inactivated fetal calf serum (Gibco), penicillin (100 U/mL), streptomycin (100 μg/mL), and 2 mM Glutamax. Mice were inoculated subcutaneously with 5×10^6 cells in 100 μL sterile PBS and were used 7−10 days after tumor inoculation, when the tumors reached approximately 70−200 mm^3 in size. At the end of each experiment the mice were anesthetized and euthanized by cervical dislocation. Blood was withdrawn by heart puncture and select organs and tissues were harvested and blotted dry. All samples were weighed and then combined with 1 mL PBS. The sample radioactivity was counted in a gamma counter (Wizard 1480, PerkinElmer) along with standards to determine the percent injected dose per gram (% ID/g) or per organ (% ID/organ).

In Vivo Stability of mAb-Conjugated TCOs. Groups of 3 tumor-free mice were administered 300 μg ^{125}I-CC49-TCO (ca. 0.8 MBq/100 μL per mouse) functionalized with 3−8 molar equiv of TCO **1**−**2** and **10** per mAb intravenously. At selected time points up to 4 days post injection, blood samples (50−60 μL) were withdrawn from the vena saphena and transferred into vials containing heparin (5 μL). The blood samples were diluted to 100 μL with PBS and reacted with an excess of carrier-added ^{177}Lu-tetrazine **13**, which was radio-labeled shortly before each experimental time point at exactly 0.2 MBq/μg specific activity. The reaction mixtures were incubated for 20 min at 37 °C and then centrifuged for 5 min at 400 × *g* to separate the blood cells. Subsequently, 30 μL of the supernatants was eluted through a Zeba desalting spin column (0.5 mL, 40 kDa MW cutoff). Mixtures containing ^{177}Lu-**13** in serum/PBS were used to determine the breakthrough of non mAb-bound ^{177}Lu from the Zeba columns (in triplicate).

The activity contained in the eluates was then measured in a gamma counter using a dual-isotope protocol (10−80 keV and 155−380 keV energy windows for ^{125}I and ^{177}Lu, respectively) with cross-contamination correction. The ^{125}I-activity was decay corrected to the injection time and the ^{177}Lu activity was corrected for ^{177}Lu-**13** breakthrough. The TCO in vivo stability was obtained by fitting the ^{177}Lu/^{125}I ratios plotted vs. the time postinjection normalized to 100% at t = 0 (Supporting Information Figure S21−S23). At the end of the evaluation, the mice were euthanized, and the ^{125}I-activity in stomachs and

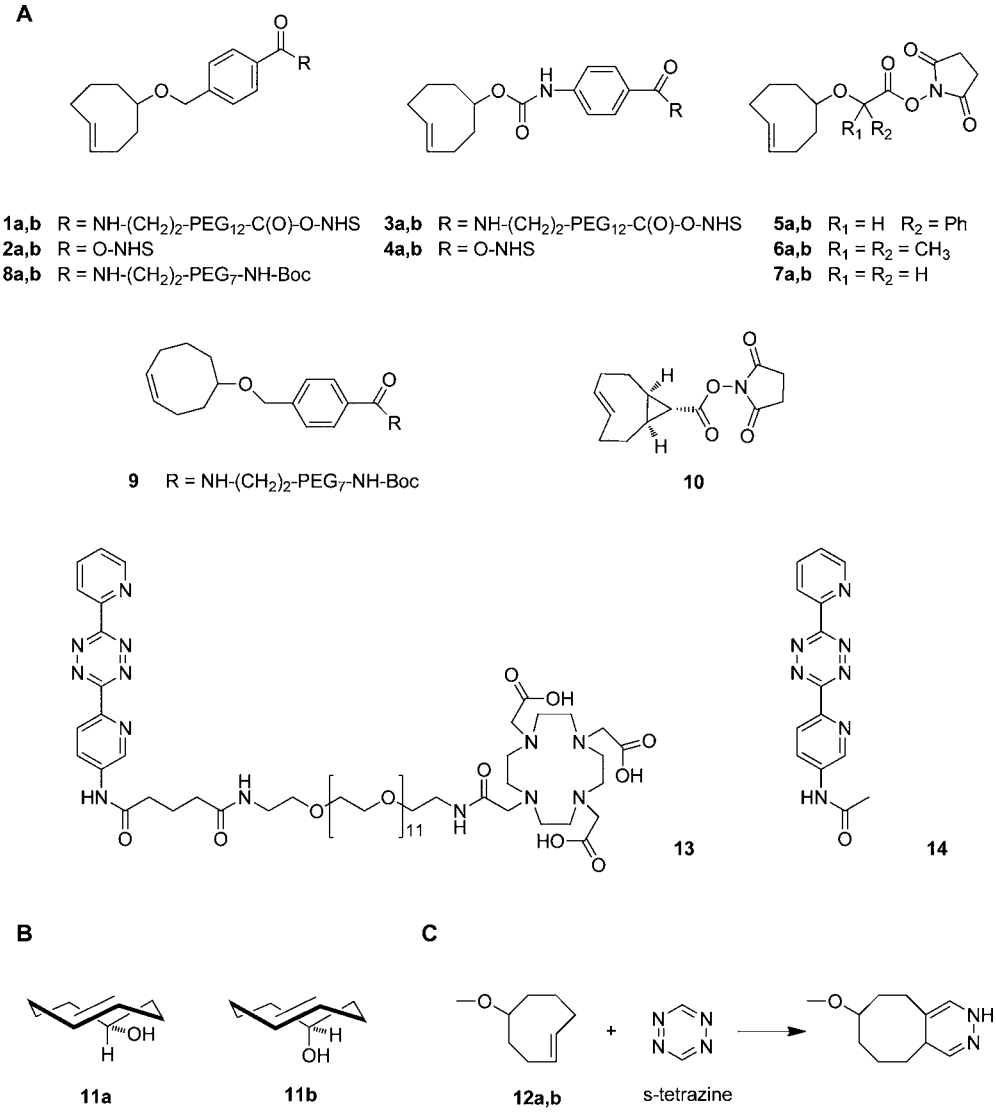

Figure 2. (a) Compounds used in the study (**a** = equatorially substituted *trans*-cyclooctenes; **b** = axially substituted *trans*-cyclooctene). (b) Equatorial (**11a**) and axial isomer (**11b**) of *trans*-cyclooct-4-enol. (c) Reaction of (*E*)-5-methoxycyclooct-1-ene (**12a,b**) with *s*-tetrazine, used in Density Functional Theory calculations.

thyroids was measured to exclude ^{125}I-CC49-TCO in vivo dehalogenation (Supporting Information Table S5).

Imaging Studies. Mice bearing LS174T xenografts were injected with CC49-TCO (**2b**) (100 μg/0.67 nmol/100 μL per mouse, carrying an average of 10.6 TCOs per mAb) followed 72 h later by ^{111}In-labeled **13** (16.7 nmol/80 μL; 36−40 MBq; 25 equiv to mAb). Approximately 90 min post-tetrazine injection the mice were anesthetized with isoflurane and imaged on a dedicated small animal SPECT/CT system (NanoSPECT/CT, Bioscan) equipped with 4 detector heads and converging 9-pinhole collimators (1.4 mm diameter). After the scan, the mice were allowed to recover and were euthanized 3 days later by anesthesia overdose. High resolution SPECT/CT scan was performed post-mortem. The SPECT images were reconstructed using HiSPECTNG (SciVis GMBH) and the data were quantitatively evaluated by drawing volumes of interest (VOI) in tumor, kidneys, liver, and thigh muscle using InVivoScope (Bioscan).

Data Analysis. The in vitro TCO degradation half-lives were calculated from the linear regression of the data or by fitting the data to a one-phase exponential decay curve. When fitting was not possible, the curves were integrated by the trapeze method and the half-life was calculated from the area under the curve (AUC) as $t_{1/2} = \ln 2 \times (AUC/C_0)$. The differences between two data points were evaluated with two-tailed unpaired *t* tests. All calculations where performed with GraphPad Prism v 4.1.

Note. Lutetium-177 and Indium-111 emit ionizing radiation (β^- and/or γ): researchers must handle them according to the guidelines set forth by their institution and national nuclear regulatory commission and follow ALARA (As Low As Reasonably Achievable) protocols to minimize exposure.

RESULTS AND DISCUSSION

To improve the in vivo stability of the TCO tag we investigated the deactivation mechanism of the previously used CC49-TCO (**1a**),[14] which was prepared by the conjugation of TCO-NHS ester **1a** (Figure 2A) to CC49 mAb lysine residues. To rule out the possibility that the tag deactivation was due to cleavage of the tag from the antibody, the pI of ^{125}I-labeled CC49-TCO (**1a**) was followed in serum at 37 °C, confirming that the

dx.doi.org/10.1021/bc400153y | *Bioconjugate Chem.* 2013, 24, 1210−1217

conjugate remained intact for 48 h (Supporting Information Figure S15–S17). We then prepared TCO model compound **8a** (Figure 2a) and incubated it in serum in the dark at 37 °C, monitored with LC-MS. We anticipated finding that the TCO was being deactivated through nucleophilic addition reactions with, e.g., thiols, as previously seen with azide-reactive cyclooctynes.[28−30] To our surprise, we found a clean conversion from *trans*-cyclooctene **8a** into *cis*-cyclooctene (CCO) **9** as the sole deactivation pathway in serum (Figure 3 and Supporting Information Figure S12). The conversion has

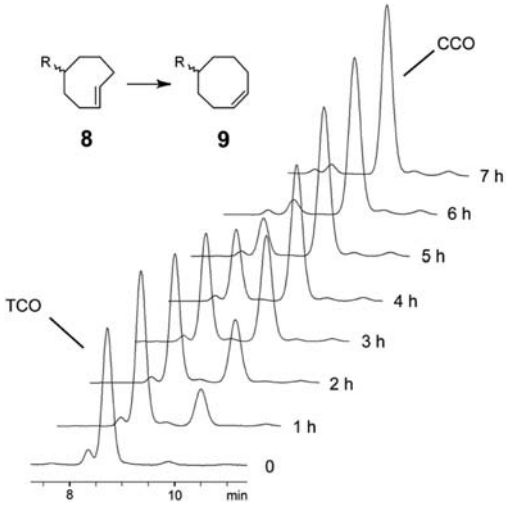

Figure 3. In vitro stability of model TCOs. Extract of HPLC profiles showing the *trans-cis* conversion of TCO **8a** to CCO **9** with time in 50% fresh mouse serum at 37 °C.

a half-life of 3.26 and 0.83 h for fresh and commercial mouse serum, respectively, while in PBS at 37 °C TCO **8a** was stable for more than one week (Table 1). As *cis*-cyclooctene is 5

Table 1. In Vitro Stability (half-life) of TCOs 8a,b in Various Media and in the Presence of Serum Components

medium	8a	8b
Fresh MS[a]	3.26 h	3.36 h
Commercial MS[a]	0.83 h	0.80 h
Transcuprein[a]	1.39 h	-
MSA[a]	0.65 h	-
MD-MSA[a]	2.84 h	-
Ceruloplasmin[b]	6.25 d	-
Transferrin[b]	stable[c]	-
Vitamine B12[b]	stable[c]	-
PBS[b]	stable[c]	-

[a]n = 3. [b]Data fitted on a 7 day scale. [c]Stable for at least 7 days.

orders of magnitude less reactive toward electron-deficient tetrazines than *trans*-cyclooctene,[31] this finding is consistent with the observed loss of reactivity in vivo. While it is known that the isomerization of *trans*-cyclooctene to *cis*-cyclooctene can be induced thermally,[32,33] by light,[34] or in concentrated thiol solutions,[21] these conditions did not apply to our experiments. In addition, reactive oxygen species are an unlikely cause of the in vivo deactivation considering the absence of oxidation products in the serum incubation experiment of model TCO **8a**.[35]

Given their role in redox reactions, we hypothesized that the deactivation in vivo was due to *trans-cis* isomerization of cyclooctene by a transition metal present in serum and accessible to the tagged antibody. As these metals are nearly exclusively bound to biomolecules, we examined the effect of five distinct and prominent serum-derived metal-containing biomolecules on the isomerization of TCO **8a** in PBS solutions corresponding to their concentration in vivo (Table 1). Transferrin (i.e., iron)[36] and vitamin B12 (i.e., cobalt)[37] were completely unreactive toward TCO **8a**, but ceruloplasmin (i.e., copper)[38] slowly isomerized **8a** with a half-life of 6.25 days. Remarkably, transcuprein and MSA, accounting for the remaining copper and the major sources of zinc,[23,38−40] very rapidly isomerized TCO **8a** to CCO **9** in half-lives of, respectively, 1.39 and 0.65 h, matching the values observed for serum. To learn if protein-bound copper or zinc indeed play a role, the experiment was repeated with MD-MSA, which had a reduced metal content from 2.88 to 0.62 mol % for copper and 2.18 to 0.07 mol % for zinc (Supporting Information Table S1). Intriguingly, MD-MSA indeed showed a slower, 4.4-fold, isomerization of **8a** (Table 1), which correlated well with the 4.6-fold reduction in copper in MD-MSA compared to MSA, suggesting a role for protein-bound copper. This was supported by a comparison of the isomerization efficiency of MD-MSA complexed with 1 equiv of Cu(II) vs Zn(II), in which the Cu-MD-MSA exhibited a 12-fold faster isomerization than Zn-MD-MSA (Supporting Information Table S2).

Copper is well-known to engage in one-electron oxidation−reduction conversions, and as such is essential for many biological processes.[38] Its activity is highly regulated through strong and specific interactions with a range of biomolecules. Transcuprein and albumin are both involved in copper transport[23,41] and rapidly isomerize **8a**, as opposed to ceruloplasmin, whose copper atoms do not belong to the exchangeable copper pool.[42] Although it is generally accepted that protein-sequestered copper is largely redox-inactive, at least for albumin it strongly depends on the oxidation state and conformation of the protein, which can affect the copper environment.[24,43,44] Oxidation of cysteine-34, in the vicinity of the copper binding site, has been shown to transform albumin from an antioxidant to a copper-based prooxidant,[44] which is consistent with reports linking albumin oxidation to reduced copper affinity[24] and albumin glycation to redox activity.[43] It may be possible that TCO engages in a redox-interaction with protein-bound Cu(II), leading to a decrease in double bond character and concomitant isomerization driven by the 10.1 kcal/mol strain energy difference[45] between *trans*- and *cis*-cyclooctene. Potential precedents for such a mechanism exist in the realms of copper-zeolite-catalyzed olefin isomerizations.[46] A possible alternative may be that the copper activates another albumin entity such as cysteine-34 and derivatives.

We postulated that the TCO could be stabilized by removal of the PEG linker between the TCO and the lysine residue on the mAb, thus increasing the steric hindrance on the TCO, which should interfere with its interaction with serum protein-bound copper. Accordingly, TCO building block **2a** (Figure 2A) was directly conjugated to the CC49 mAb. A subsequent stability assay in circulation in mice gratifyingly revealed a striking increase in TCO half-life from 2.62 to 6.19 days (Table 2). In addition, the reactivity of CC49-TCO (**2a**) toward tetrazine probe **13** was not compromised by the removal of the linker, as evidenced by a retained high second order rate constant of $(3.2 \pm 0.2) \times 10^4$ M^{-1} s^{-1} (Table 2).

Table 2. Left: Reaction Kinetics between CC49-Conjugated TCOs (1a,b−7a,b and 10) and ^{177}Lu-Tetrazine 13 Measured in PBS at 37 °C. Right: In Vivo Stability of CC49-Conjugated TCOs (1a,b−2a,b and 10) in Non-Tumor Bearing Mice (n = 3)[a]

	k_2 ($\times 10^4$ M^{-1} s^{-1})		in vivo stability half-life (days)	
TCO	equatorial (**a**)	axial (**b**)	equatorial (**a**)	axial (**b**)
1	2.7 ± 0.2	26.1 ± 0.5	2.62	1.12
2	3.2 ± 0.2	27.3 ± 0.5	6.19	3.94
3	2.5 ± 0.1	17.9 ± 0.3	--	--
4	1.3 ± 0.1	10.0 ± 1.3	--	--
5	2.9 ± 0.2	16.3 ± 0.3	--	--
6	2.5 ± 0.4	14.8 ± 1.2	--	--
7	2.1 ± 0.0	13.5 ± 0.1	--	--
10	280 ± 8		0.67	

[a]Half-lives obtained from linear regression (**1a**, **2a**,**b**, **10**) or one-phase decay fitting (**1b**) of the data (0 to 4 days).

We speculated that the increased stability due to the improved conjugate design should afford sufficient compensation for the anticipated TCO destabilization when working toward tags with increased reactivity. Fox and co-workers described an elegant approach for a highly reactive TCO derivative in a 'half-chair' conformation (**10**, Figure 2A), based on bicyclo[6.1.0]non-4-ene, which has successfully been used in bioconjugations in vitro.[21] However, a subsequent study found that this motif possibly suffers from intrinsic instability.[10] When we prepared a conjugate of **10** with CC49 and evaluated its reactivity in PBS and its stability in circulation in mice, we found a high second order constant but also a relatively rapid and unpractical in vivo deactivation (k_2 = 2.8 × 10^6 M^{-1} s^{-1} in PBS; half-life = 0.67 d; Table 2). The favored, lower energy, conformation for the parent *trans*-cyclooctene, as well as the widely used *trans*-cyclooct-4-enol **11** and its derivatives, is the crown conformation (Figure 2B).[47] While the hydroxyl substituent in **11** can be either in the equatorial or axial position within this crown conformation, the photolysis-based synthesis of **11** from (*Z*)-cyclooct-4-enol predominantly leads to the equatorial isomer **11a** (**11a**/**11b** ratio: 2.2), as, in general, axially substituted ring systems are higher in energy due to trans-annular interactions.[47] We realized that the higher energy harnessed in TCO derivatives with axial substituents may provide an entry to tags with a significantly increased reactivity and therefore developed a series of TCO tags containing axially positioned bulky linkers. Starting from the hydroxyl group of the axial isomer **11b**, which can be obtained in 24% yield after column chromatography purification of the mixture of diastereomers **11**,[47] we prepared derivatives comprising benzyl ether (**2b**), phenylcarbamate (**4b**), 2-alkoxy-2-phenylacetate (**5b**), and 2-alkoxy-2-methylpropanoate (**6b**) linker moieties. For comparison purposes, **2b** and **4b** were also prepared as PEG conjugates **1b** and **3b**, respectively, alkoxyacetate TCO **7b** was included,[47] and all TCO tags were also prepared as the equatorial isomer starting from **11a** (Figure 2A). The active esters **1**−**7a**,**b** were conjugated to CC49 mAb via the lysine residues and the reaction kinetics of the mAb-bound TCOs were assessed in reaction with ^{177}Lu-tetrazine probe **13** (Table 2 and Supporting Information Figure S18). Perusal of Table 2 clearly shows that the increased strain energy in the axial isomers translates to a markedly increased reactivity. The most reactive axial TCO was the bulky benzyl ether linked TCO **2b** with a k_2 = (27.3 ± 0.5) × 10^4 M^{-1} s^{-1}, which is 9- to 10- fold more reactive than **1a** and **2a**. We also studied the reaction between *trans*-cyclooct-4-enol **11** with tetrazine **14**, a truncated analog of **13** (Figure 2A), and found k_2 = (1.4 ± 0.0) × 10^4 M^{-1} s^{-1} for **11a** and a 5.5-fold higher k_2 = (7.9 ± 0.1) × 10^4 M^{-1} s^{-1} for **11b** in water (Supporting Information Figure S19 and Table S4). This matches Density Functional Theory calculations (Supporting Information) giving a 5-fold higher reactivity of the axial compared to the equatorial isomer of (E)-5-methoxycyclooct-1-ene (**12a**,**b**) in reaction with *s*-tetrazine (Figure 2C). The fact that the values for **11** correspond to the least reactive TCOs in Table 2, and that for most TCOs in Table 2 the equatorial-axial reactivity difference is slightly larger than 5.5 (up to 10), is likely due to the desired additional axial interactions of the TCO ring with the linker moieties of **1**−**7**, not present in **11**. During our studies, Jäschke and co-workers reported the successful application of the inv-DA reaction and the copper-catalyzed azide−alkyne click reaction for mutually orthogonal conjugation reactions with DNA.[48] In this study, they observed a 3.2-fold reactivity difference between the equatorial and axial isomer of the phosporamidite derivative of TCO **11**, which, even though there are differences in used tetrazine and reaction medium, is slightly lower than expected on the basis of the results for TCO **1**−**7**.

Axial TCO **2b** was selected for further evaluation and we confirmed that the higher reactivity of **2b** vs **2a** translates to higher yields (5.4-fold at 10 nM) when reacted with an equal amount ^{177}Lu-**13** at the much reduced, low nM, reagent concentrations, which have to be overcome when extending the scope from mice to larger animals and humans (Supporting Information Figure S20). Next, model compound **8b** (Figure 2A) was prepared to study its fate in serum, analogous to equatorial **8a**. Again, the only observed deactivation pathway in serum was a clean *trans*−*cis* isomerization, with no evidence of side reactions (Supporting Information Figure S13). Subsequent assessment of the in vivo stability of CC49-conjugated **2b** and its PEG-linked analog **1b** in circulation in mice revealed a half-life of 1.12 days for **1b** and a nearly 4-fold slower deactivation for **2b** with a half-life of 3.94 days (Table 2). The combined efforts of increasing the stability and reactivity resulted in TCO tag **2b** with a 10-fold increased reactivity and a 1.5-fold improved stability compared to the previously used **1a**.

To test the on-tumor stability of the CC49-bound-TCO (**2b**) and its inv-DA reaction product, we carried out a pretargeted SPECT/CT imaging experiment in mice (n = 3) bearing LS174T colon carcinoma xenografts using an extended, 3 days vs 1, interval between CC49-TCO and ^{111}In-tetrazine **13**, and by monitoring the mice for another 3 days (Figure 4 and Supporting Information Figure S24). Compared to the 1-day interval used in our previous work,[14] the images of the live mice acquired shortly after tetrazine injection have a lower background due to less CC49-TCO circulating in blood after 3 days, and again show a pronounced radioactivity uptake in the tumor (3.18 ± 0.29% ID/g) (Figure 4A). The latter finding reflects the similar amounts of remaining intact TCO after 3 days in vivo for the improved **2b** vs 1 day for the parent **1a** (respectively, 60% and 75%). Corresponding dual isotope biodistribution experiments confirmed the SPECT/CT results (Supporting Information Tables S6 and S7). Remarkably, when the live mice were imaged again 3 days later, the radioactivity in the tumor (2.22 ± 0.32% ID/organ) was unchanged from the first scan (2.12 ± 0.30% ID/organ) (Figure 4B). As the TAG-72 antigen to which CC49 binds is relatively stable on the outside of the cell,[49] this finding indicates that the inv-DA

dx.doi.org/10.1021/bc400153y | *Bioconjugate Chem.* 2013, 24, 1210−1217

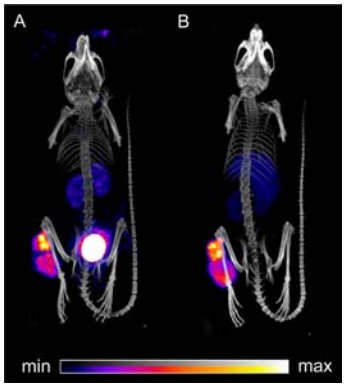

Figure 4. Small-animal SPECT/CT imaging of one mouse bearing a colon carcinoma xenograft preinjected with 100 μg CC49-TCO (**2b**) followed 72 h later by ^{111}In-tetrazine **13** (25 equiv to mAb, 40 MBq): posterior projections (A) 1.5 h and (B) 3 days post-tetrazine injection (post-mortem).

reaction product is at least largely stable in vivo for days, which together with the fact that tetrazine **13** is only retained in TCO-containing tissues, is highly beneficial with respect to delivering high tumor doses during pretargeted RIT.

CONCLUSION

To increase the potential of in vivo chemistry with the inv-DA reaction, we set out to increase its reactivity without compromising reagent stability. In doing so, we discovered that the TCO tag is potentially deactivated in vivo by its interaction with copper-containing proteins, which was counteracted by shortening of the TCO linker. Next, we found that the higher reactivity of axial vs equatorial linked TCO can be augmented by the choice of linker. The combination of both findings afforded a 10-fold more reactive TCO with increased in vivo stability, allowed for effective on-tumor reactivity and an increase of T/B ratios in mice. The achieved TCO reactivity is close to the range of association rates for the biological interactions, possibly allowing for organic chemistry in larger animals and eventually humans.

ASSOCIATED CONTENT

Supporting Information

Materials and Methods; Synthesis; and Biodistribution Studies. This material is available free of charge via the Internet at http://pubs.acs.org.

AUTHOR INFORMATION

Corresponding Author

*Phone: +31402748264. Fax: + 31402744906. E-mail: marc.robillard@tagworkspharma.com.

Notes

The authors declare the following competing financial interest(s): Tagworks shareholder.

ACKNOWLEDGMENTS

We thank Dr. Nico Willard for insightful discussions, Erica Aussems-Custers, Pascal Renart-Verkerk, and Sidney Wessels for support with chemical synthesis; Hugo Knobel and Jeanette Smulders for respectively HRMS and ICP-MS measurements; Dr. Iris Verel, Monique Berben, Caren van Kammen, Carlijn van Helvert, and Melanie Blonk for support with in vivo experiments; and Dr. Reinder Coehoorn and Scientific Computing & Modelling (SCM) for use of the ADF software.

ABBREVIATIONS

% ID/g, percent injected dose per gram; % ID/organ, percent injected dose per organ; BCA assay, bicinchoninic acid assay; BSA, bovine serum albumin; CCO, *cis*-cyclooctene; DOTA, 1,4,7,10-tetraazacyclododecane-1,4,7,10-tetraacetic acid; DTPA, diethylenetriamine pantaacetic acid; EDTA, ethylenediamine tetraacetic acid; IEF, isoelectric focusing; inv-DA, inverse-electron-demand Diels−Alder; ITLC, instant thin layer chromatography; pI, isoelectric point; MD-MSA, metal depleted mouse serum albumin; MSA, mouse serum albumin; RIT, radioimmunotherapy; RP-HPLC, reverse phase HPLC; SDS-PAGE, sodium dodecyl sulfate polyacrylamide gel electrophoresis; SEC, size exclusion chromatography; SHPP, N-succinimidyl-3-(4-hydroxyphenyl)propionate; TCO, *trans*-cyclooctene

REFERENCES

(1) Debets, M. F., Van Berkel, S. S., Dommerholt, J., Dirks, A. J., Rutjes, F. P. J. T., and Van Delft, F. L. (2011) Bioconjugation with strained alkenes and alkynes. *Acc. Chem. Res. 44*, 805−815.

(2) Devaraj, N. K., and Weissleder, R. (2011) Biomedical applications of tetrazine cycloadditions. *Acc. Chem. Res. 44*, 816−827.

(3) Sletten, E. M., and Bertozzi, C. R. (2011) From mechanism to mouse: a tale of two bioorthogonal reactions. *Acc. Chem. Res. 44*, 666−676.

(4) Boerman, O. C., van Schaijk, F. G., Oyen, W. J. G., and Corstens, F. H. M. (2003) Pretargeted Radioimmunotherapy of Cancer: Progress Step by Step. *J. Nucl. Med. 44*, 400−411.

(5) Chatal, J. F., Davodeau, F., Cherel, M., and Barbet, J. (2009) Different ways to improve the clinical effectiveness of radio-immunotherapy in solid tumors. *J. Cancer Res. Ther. 5*, 36−40.

(6) Goldenberg, D. M., Sharkey, R. M., Paganelli, G., Barbet, J., and Chatal, J.-F. (2006) Antibody pretargeting advances cancer radio-immunodetection and radioimmunotherapy. *J. Clin. Oncol. 24*, 823−834.

(7) Aweda, T. A., Beck, H. E., Wu, A. M., Wei, L. H., Weber, W. A., and Meares, C. F. (2010) Rates and equilibria for probe capture by an antibody with infinite affinity. *Bioconjugate Chem. 21*, 784−791.

(8) Liu, G., Mang'era, K., Liu, N., Gupta, S., Rusckowski, M., and Hnatowich, D. J. (2002) Tumor pretargeting in mice using ^{99m}Tc-labeled Morpholino, a DNA analog. *J. Nucl. Med. 43*, 384−391.

(9) Blackman, M. L., Royzen, M., and Fox, J. M. (2008) Tetrazine ligation: fast bioconjugation based on inverse-electron-demand Diels-Alder reactivity. *J. Am. Chem. Soc. 130*, 13518−13519.

(10) Lang, K., Davis, L., Wallace, S., Mahesh, M., Cox, D. J., Blackman, M. L., Fox, J. M., and Chin, J. W. (2012) Genetic encoding of bicyclononynes and *trans*-cyclooctenes for site-specific protein labeling in vitro and in live mammalian cells via rapid fluorogenic Diels-Alder reactions. *J. Am. Chem. Soc. 134*, 10317−10320.

(11) Zeglis, B. M., Mohindra, P., Weissmann, G. I., Divilov, V., Hilderbrand, S. A., Weissleder, R., and Lewis, J. S. (2011) Modular strategy for the construction of radiometalated antibodies for positron emission tomography based on inverse electron demand Diels-Alder click chemistry. *Bioconjugate Chem. 22*, 2048−2059.

(12) Devaraj, N. K., Upadhyay, R., Haun, J. B., Hilderbrand, S. A., and Weissleder, R. (2009) Fast and sensitive pretargeted labeling of cancer cells through a tetrazine/trans-cyclooctene cycloaddition. *Angew. Chem., Int. Ed. 48*, 7013−7016.

(13) Li, Z., Cai, H., Hassink, M., Blackman, M. L., Brown, R. C. D., Conti, P. S., and Fox, J. M. (2010) Tetrazine-*trans*-cyclooctene ligation for the rapid construction of ^{18}F labeled probes. *Chem. Commun. 46*, 8043−8045.

(14) Rossin, R., Renart Verkerk, P., van den Bosch, S., Vulders, R., Verel, I., Lub, J., and Robillard, M. (2010) In vivo chemistry for

pretargeted tumor imaging in live mice. *Angew. Chem., Int. Ed. 49*, 3375−3378.
(15) Schlom, J., Eggensperger, D., Colcher, D., Molinolo, A., Houchens, D., Miller, L. S., Hinkle, G., and Siler, K. (1992) Therapeutic advantage of high-affinity anticarcinoma radioimmunoconjugates. *Cancer Res. 52*, 1067−1072.
(16) Devaraj, N. K., Thurber, G. M., Keliher, E. J., Marinelli, B., and Weissleder, R. (2012) Reactive polymer enables efficient in vivo bioorthogonal chemistry. *Proc. Natl. Acad. Sci. U.S.A.. 109*, 4762−4767.
(17) Changed value compared to ref 14 due to adapted quantification method.
(18) Green, N. M. (1963) Avidin. 1. The use of [^{14}C]biotin for kinetic studies and for assay. *Biochem. J. 89*, 585−591.
(19) Karlsson, R., Michaelsson, A., and Mattsson, L. (1991) Kinetic analysis of monoclonal antibody-antigen interactions with a new biosensor based analytical system. *J. Immunol. Methods 145*, 229−240.
(20) Orcutt, K. D., Slusarczyk, A. L., Cieslewicz, M., Ruiz-Yi, B., Bhushan, K. R., Frangioni, J. V., and Wittrup, K. D. (2010) Engineering an antibody with picomolar affinity to DOTA chelates of multiple radionuclides for pretargeted radioimmunotherapy and imaging. *Nucl. Med. Biol. 38*, 223−233.
(21) Taylor, M. T., Blackman, M. L., Dmitrenko, O., and Fox, J. M. (2011) Design and synthesis of highly reactive dienophiles for the tetrazine-*trans*-cyclooctene ligation. *J. Am. Chem. Soc. 133*, 9646−9649.
(22) Martins, E. O., and Drakenberg, T. (1982) Cadmium(II), zinc(II), and copper(II) ions binding to bovine serum albumin. A ^{113}Cd NMR study. *Inorg. Chim. Acta 67*, 71−74.
(23) Moriya, M., Ho, Y.-H., Grana, A., Nguyen, L., Alvarez, A., Jamil, R., Ackland, M. L., Michalczyk, A., Hamer, P., Ramos, D., Kim, S., Mercer, J. F. B., and Lindner, M. C. (2008) Copper is taken up efficiently from albumin and α2-macroglobulin by cultured human cells by more than one mechanism. *Am. J. Physiol. Cell Physiol. 295*, C708−C721.
(24) Zhang, Y., and Wilcox, D. E. (2002) Thermodynamic and spectroscopic study of Cu(II) and Ni(II) binding to bovine serum albumin. *J. Biol. Inorg. Chem. 7*, 327−337.
(25) Bal, W., Christodoulou, J., Sadler, P. J., and Tucker, A. (1998) Multi-metal binding site of serum albumin. *J. Inorg. Biochem. 70*, 33−39.
(26) Blindauer, C. A., Harvey, I., Bunyan, K. E., Steward, A. J., Sleep, D., Harrison, D. J., Berezenko, S., and Sadler, P. J. (2009) Structure, properties, and engineering of the major zinc binding site on human albumin. *J. Biol. Chem. 284*, 23116−23124.
(27) Sadler, P. J., Tucker, A., and Viles, J. H. (1994) Involvement of a lysine residue in the N-terminal Ni^{2+} and Cu^{2+} binding site of serum albumins. Comparison with Co^{2+}, Cd^{2+} and Al^{3+}. *Eur. J. Biochem. 220*, 193−200.
(28) Chang, P. V., Prescher, J. A., Sletten, E. M., Baskin, J. M., Miller, I. A., Agard, N. J., Lo, A., and Bertozzi, C. R. (2010) Copper-free click chemistry in living animals. *Proc. Natl. Acad. Sci. U.S.A. 107*, 1821−1826.
(29) van Geel, R., Pruijn, G. J. M., van Delft, F. L., and Boelens, W. C. (2012) Preventing thiol-yne addition improves the specificity of strain-promoted azide-alkyne cycloaddition. *Bioconjugate Chem. 23*, 392−398.
(30) van den Bosch, S. M., Rossin, R., Renart Verkerk, P., ten Hoeve, W., Janssen, H. M., Lub, J., and Robillard, M. S. (2013) Evaluation of strained alkynes for Cu-free click reaction in live mice. *Nucl. Med. Biol. 40*, 415−423.
(31) Thalhammer, F., Wallfahrer, U., and Sauer, J. R. (1990) Reaktivität einfacher offenkettiger und cyclischer dienophile bei Diels-Alder-reaktionen mit inversem elektronenbedarf. *Tetrahedron Lett. 31*, 6851−6854.
(32) Cope, A. C., and Pawson, B. A. (1965) Molecular asymmetry of olefins. IV. Kinetics of racemization of (+ or -)-*trans*-cyclooctene. *J. Am. Chem. Soc. 87*, 3649−3651.
(33) Holle Andrews, U., Baldwin, J. E., and Grayston, M. W. (1982) On the thermal isomerization of trans-cyclooctene to cis-cyclooctene. *J. Org. Chem. 47*, 287−292.
(34) Inoue, Y., Kobata, T., and Hakushi, T. (1985) Reinvestigation of triplet-sensitized cis-trans photoisomerization of cyclooctene. Alkene-concentration and sensitizer-ET dependence of photostationary *trans*/*cis* ratio. *J. Phys. Chem. 89*, 1973−1976.
(35) Valko, M., Leibfritz, D., Moncol, J., Cronin, M. T. D., Mazur, M., and Telser, J. (2007) Free radicals and antioxidants in normal physiological functions and human disease. *Int. J. Biochem. Cell Biol. 39*, 44−84.
(36) Lindley, P. F. (2001) Transferrins, in *Handbook of metalloproteins* (Messerschmidt, A., Huber, R., Wieghardt, K., and Poulos, T., Eds.) pp 793−810, John Wiley & Sons, Ltd, Chichester.
(37) Anderson, B. B. (1964) Investigations into Euglena method for the assay of the vitamin B12 in serum. *J. Clin. Pathol. 17*, 14−26.
(38) Crisponi, G., Nurchi, V. M., Fanni, D., Gerosa, C., Nemolato, S., and Faa, G. (2010) Copper-related diseases: From chemistry to molecular pathology. *Coord. Chem. Rev. 254*, 876−889.
(39) Cabrera, A., Alonzo, E., Sauble, E., Chu, Y. L., Nguyen, D., Lindner, M. C., Sato, D. S., and Mason, A. Z. (2008) Copper binding components of blood plasma and organs, and their responses to influx of large doses of ^{65}Cu, in the mouse. *Biometals 21*, 525−543.
(40) Foote, J. W., and Delves, H. T. (1984) Albumin bound and alpha-2-macroglobulin bound zinc concentrations in the sera of healthy adults. *J. Clin. Pathol. 37*, 1050−1054.
(41) Peters, T. J. (1996) The Albumin Molecule: Its Structure and Chemical Properties, in *All about Albumin: Biochemistry, Genetics and Medical Applications*, pp 9−54, Academic Press, New York.
(42) Lindley, P. F. (2001) Ceruloplasmin, in *Handbook of metalloproteins* (Messerschmidt, A., Huber, R., Wieghardt, K., and Poulos, T., Eds.) pp 1369−1380, John Wiley & Sons, Ltd, Chichester.
(43) Argirova, M. D., and Ortwerth, B. J. (2003) Activation of protein-bound copper ions during early glycation: study on two proteins. *Arch. Biochem. Biophys. 420*, 176−184.
(44) Gryzunov, Y. A., Arroyo, A., Vigne, J.-L., Zhao, Q., Tyurin, V. A., Hubel, C. A., Gandley, R. E., Vladimirov, Y. A., Taylor, R. N., and Kagan, V. E. (2003) Binding of fatty acids facilitates oxidation of cysteine-34 and converts copper−albumin complexes from antioxidants to prooxidants. *Arch. Biochem. Biophys. 413*, 53−66.
(45) Bach, R. D. (2009) Ring strain energy in the cyclooctyl system. The effect of strain energy on [3 + 2] cycloaddition reactions with azides. *J. Am. Chem. Soc. 131*, 5233−5243.
(46) John, C. S., and Leach, H. F. (1977) Determination of the active site and mechanism for alkene isomerization in CuII exchanged Y-type zeolite. *J. Chem. Soc., Faraday Trans. 1* (73), 1595−1604.
(47) Royzen, M., Yap, G. P. A., and Fox, J. M. (2008) A photochemical synthesis of functionalized *trans*-cyclooctenes driven by metal complexation. *J. Am. Chem. Soc. 130*, 3760−3761.
(48) Schoch, J., Staudt, M., Samanta, A., Wiessler, M., and Jäschke, A. (2012) Site-specific one-pot dual labeling of DNA by orthogonal cycloaddition chemistry. *Bioconjugate Chem. 23*, 1382−1386.
(49) Katari, R. S., Fernsten, P. D., and Schlom, J. (1990) Characterization of the shed form of the human tumor-associated glycoprotein (TAG-72) from serous effusions of patients with different types of carcinomas. *Cancer Res. 50*, 4885−4890.